

# SHEAR STRENGTH OF 160 MPa STEEL FIBRE REINFORCED REACTIVE POWDER CONCRETE BRIDGE GIRDERS WITHOUT STIRRUPS

Jackie Voo Yen Lei

B.E (Civil), PhD (Structure)

E-mail: vooyenlei@dura.com.my

## ABSTRACT

The development of ultra-high-strength-high-performance concrete known as the reactive powder concrete (RPC) was originated in the mid 1990's by the French and now commercialised under the trade name of DUCTAL by Lafarge-Bouygues-Rhodia, CERACEM by Eiffage and CEMTEC by LCPC. Although RPC has a decade of history with many proven projects and astonishing landmarks have been mounted at various parts of the world, the demand of RPC has yet to be established in this country. This paper shows some of the significant potential advantages of using fibre reinforced RPC in bridge engineering. Experimental results on testing of seven prototype 650 mm deep large-scale I-section girders failing in shear were reported herein. The girders were casted using 150-170 MPa steel fibre reinforced reactive powder concrete and were designed to assess the ability of steel fibre reinforced reactive powder concrete (SFR-RPC) to carry shear stresses in thin webbed prestressed beams without shear reinforcement. Experimental results showed that the quantities and types of fibres in the concrete mix do not significantly affect the initial shear cracking load but increasing the volume of fibers increased the failure load.

**Keywords :** Prestressed Beam, Shear, Steel Fiber, Thin Web

## 1 INTRODUCTION

The terminology of ultra-high-performance concrete (UHPC) is not new anymore for many today's concrete researchers. However, the demand and acknowledgement on this revolutionary material has yet to be established in Malaysia and also in many other countries in the world.

These mentioned UHPC, also widely known as the reactive powder concrete (RPC) is a revolutionary material developed by the French in the mid 1990's when Richard and Cheyrezy [1, 2] produced concrete-mortar with compressive strengths and modulus of rupture in excess of 200 MPa and 25 MPa, respectively. Today this material is commercialised under the trade name of DUCTAL by Lafarge-Rhodia-Bouygues, CERACEM by Eiffage and CEMTEC by LCPC.

A decade has passed with many completed projects have been mounted and proven the uniqueness of RPC as revolutionaries building material; instead of merely a "close-door" laboratory invention. Many successful applications of RPC have been reported such the 60 meter span Sherbrooke footbridge in Canada (1997); the Cattenom power station in France (1999); 7 meter span roof panels in USA (2001); the 120 meter span Seonyu footbridge in South Korea (2002); the 50 meter span Sakata Mirai footbridge in Japan (2002); the Shawnessy LRT station canopy in Canada (2003); the 16 meter span Shepherd Gully Creek Bridge in Australia (2004); the 25 meter span Futur Bridge in USA (2005) and many others.

For a long time, researchers/engineers anticipated to remove shear reinforcements from reinforced/prestressed concrete bridge girders in order to save cost and construction time. This anticipation seems less promising not until the technology of RPC has been developed.

So what is RPC? In brief, RPC is an ultra-high strength, low porosity, cementitious material with high cement and silica

fume contents, incorporated with high quantity of fiber, low water-binder ratio (W/B) exhibiting extraordinary characteristics in terms of strength, durability and ductility. One of the most distinctive properties of RPC is that the fracture energy ( $G_f$ ) is more than two orders of magnitude higher than conventional concrete. In short, with its superior mechanical properties and high tension failure mechanism, fiber reinforced RPC can be used to resist all but direct primary tensile stresses or localised shear. Thus, this may eliminates the need for supplemental shear and other auxiliary reinforcing steel.

The objective of this paper is to report on the experimental result of seven prototype steel fibre reinforced reactive powder concrete (SFR-RPC) prestressed I-section girders (SB1 to SB7) failing in direct tension (shear). In this paper selection of variables, specimen fabrication procedures, test configuration, instrumentation and gauging, experimental results and comments on test results are reported.

## 2 EXPERIMENTAL PROGRAMME

### 2.1. VARIABLE AND SPECIMEN DIMENSIONS

The main variables studied in the experimental program were type and quantity of fibres, and level of prestress. The girders were 4.5 meter in total length having a span of 4.0 meter and a total depth of 650 mm. The web of the girders was designed as a thin uniform membrane of 50 mm thick. The top flanges were 400 mm wide and contained 6/15.2 mm diameter high strength steel prestressing wires. The bottom flanges were 250 mm wide and contained 12/15.2 mm diameter strands.

The strand used herein are manufactured as per AS1311 [3] and has a guaranteed ultimate tensile strength (GUTS) of 1750 MPa which is equivalent to a minimum breaking load of 250 kN. The nominal cross-sectional area ( $A_p$ ) of the strand is 143 mm<sup>2</sup>.

The girder dimensions are shown in Figure 1. The specimens were designed to fail in diagonal shear in the thin web region.

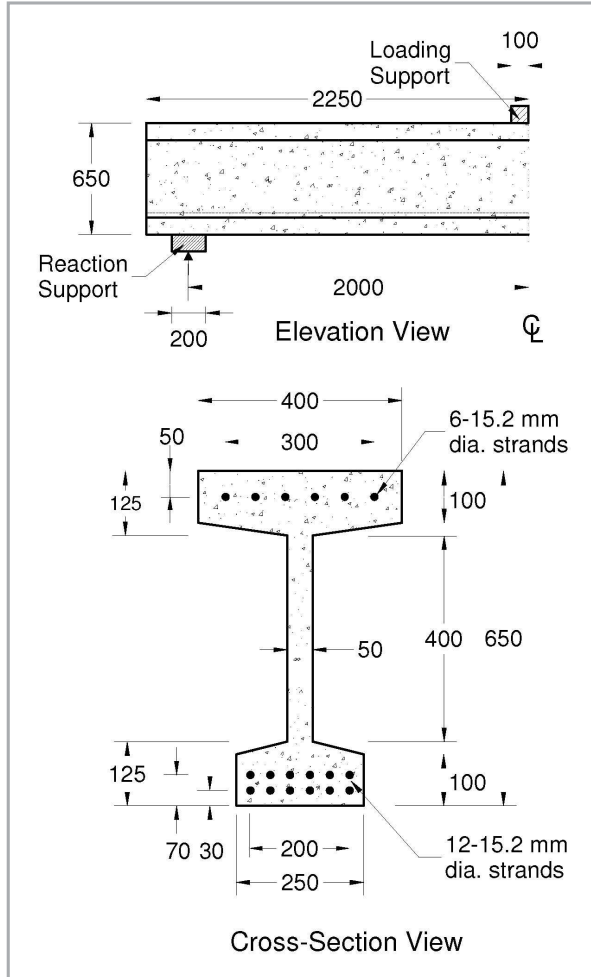


Figure 1: Steel fiber reinforced RPC prestressed girders (dimension in mm)

## 2.2. MATERIAL, MIX DESIGN AND FABRICATION

Details of the SFR-RPC mix for specimens SB1 to SB7 are given in Table 1. The SFR-RPC used in this project is produced using a high energy concrete mixer provided by VSL Prestressing (Australia). The cement used in this project was Kandos Type 1 General Portland cement manufactured to AS3972 [4]; the undensified silica fume used was produced in Western Australia and Sydney sand was used with particle size range between 150  $\mu\text{m}$  and 400  $\mu\text{m}$ . The superplasticiser used in the mix was a polycarboxylic ether based superplasticiser. Type I fibers were straight 13 mm long by 0.2 mm diameter and are fabricated from very high strength steel with minimum tensile strength of 1800 MPa. Type II fibers were end hooked fibers 30 mm long by 0.5 mm diameter and are made from high strength bright mild steel with a tensile strength of 1200 MPa. Two fiber volume ratios of 1.25 and 2.5% were used.

All the dry components (i.e. cement, silica fume and sand) were pre-batched into 0.5 tonne bags. The dry components were then transported to the high energy mixer and mixed for

Table 1: Fiber reinforced RPC mix designs for specimens SB1 to SB7- material quantities (kg per  $\text{m}^3$  of RPC)

Component	Specimen						
	SB1	SB2	SB3	SB4	SB5	SB6	SB7
GP Cement	928	920	911	939	937	911	920
Sydney sand	928	920	911	939	937	911	920
Silica fume	223	221	219	225	225	219	221
Superplasticiser	39	39	38	39	39	38	39
Steel fibers (Type I)	176	175	173	89	107	0	131
Steel fibers (Type II)	0	0	0	0	71	173	43
Total water	186	193	200	188	178	200	193
W/B	0.16	0.17	0.18	0.16	0.15	0.18	0.17
Total Fiber Volumetric Ratio (%)	2.5	2.5	2.5	1.25	2.5	2.5	2.5

about 10 minutes. Water and superplasticiser were added gradually until the materials were uniformly mixed. The fibres were introduced last, dispersed uniformly and mixing continued for a further 10 minutes. Flow table tests as per ASTM C-230 [5] was undertaken before casting of the specimen. All specimens were cast vertically in steel forms as shown in Figure 2. The forms were cleaned and greased to allow smooth stripping. The fresh SFR-RPC was compacted using external vibrators which were attached to the steel forms. Within one hour of casting, the specimens and test control samples were covered under wet hessian and plastic sheeting until the day of demoulding. After stripping, the specimens were cured for 7 days at 80°C in a hot water bath. After 9 days (12 days for specimen SB2) the specimens were removed from the hot water bath and air cured until the day of testing.



Figure 2: Pouring of fresh SFR-RPC in the girder steel forms

## 2.3. TEST SETUP AND INSTRUMENTATIONS

This experimental programme was undertaken in the heavy structural laboratory of School of Civil and Environmental Engineering of University of New South Wales (Australia). Details of the specimens, experimental variables and the test setup and instrumentation are given in Table 2 and Figure 3,

041-046·shear strength 8/30/06 12:47 PM Page 43

041-046·shear strength 8/30/06 12:47 PM Page 43

041-046·shear strength 8/30/06 12:47 PM Page 43

Table 2: Detail of specimens SB1 to SB7

Beam No.	Prestressing Force (kN)		$\sigma_{top}$ MPa	$\sigma_{bot}$ MPa	$\sigma_{av}$ MPa	Fiber Volume (%)
	Top I-flange	Bottom I-flange				
SB1	0	0	0	0	0	Type I- 2.5
SB2	450	900	-4.72	-27.2	-14.3	Type I- 2.5
SB3	225	450	-2.36	-13.6	-7.15	Type I- 2.5
SB4	225	450	-2.36	-13.6	-7.15	Type I- 1.25
SB5	225	450	-2.36	-13.6	-7.15	Type I- 1.5 Type II- 1.0
SB6	225	450	-2.36	-13.6	-7.15	Type II- 2.5
SB7	225	450	-2.36	-13.6	-7.15	Type I- 1.88 Type II- 0.62

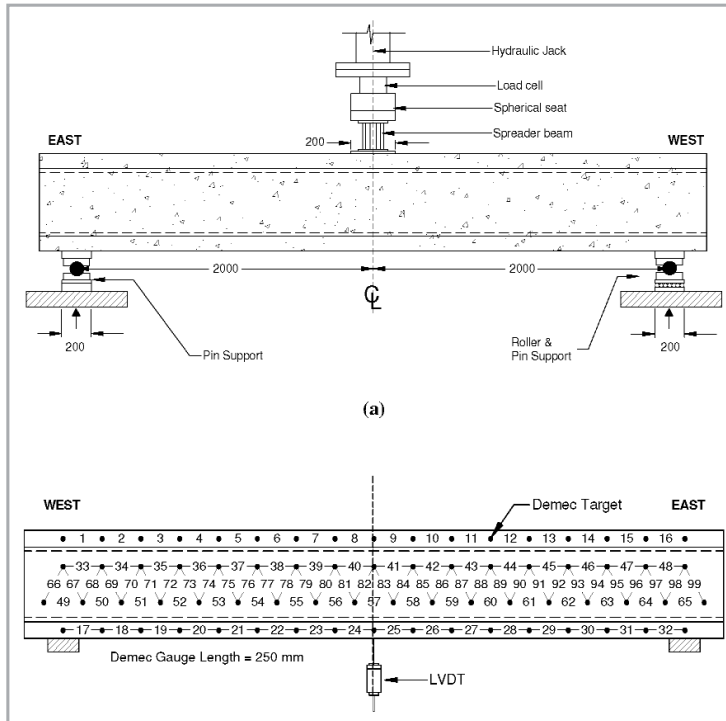


Figure 3: (a) Experimental setup and (b) location of Demec gauges and LVDT

respectively. Specimen SB3 was set as the reference specimen with 2.5% of Type I fibres and with 15% prestress (i.e. 15% of GUTS). Specimens SB3 to SB7 were prestressed to 15% of the GUTS of the strands giving an average prestress in the section of 7.2 MPa. Each strand in specimens SB1 and SB2 was prestressed to 0 and 30% of the GUTS, respectively. Specimen SB4 was similar to specimen SB3 except it had half the amount of Type I fibre in its mix. Specimen SB5 and SB7 consisted of fiber cocktail RPC mixes with varying quantities of Type I and II fibers and beam SB6 contained only 2.5% of Type II fibres.

All the specimens had a similar experimental setup and instrumental gauging (demonstrates in Figure 3). The specimens were simply supported over a 4 meter span (measured between support centrelines) and the applied concentrated load was placed at the centre of the specimens. All specimens were tested in a 5000 kN capacity stiff testing frame and tested under ram displacement control (see Figure 4).

One end of each specimen was a pinned support and the other end had a pin and roller support. The pins and rollers were greased to minimise friction and to give free rotation and horizontal translation, as required. The instrumentation used

for each specimen is shown in Figure 3b with monitoring of 99 sets of Demec (DM) gauges and a LVDT. DMs 1 to 16 were located at the top (compression) flange of the specimen with DMs 17 to 32 located at the bottom (tension) flange. Demec gauges 33 to 99 were located in the web regions of the specimens to measure longitudinal and shear strains in the web.

The displacement transducer LVDT was placed to measure the midspan displacement of the beam. Load was applied in increment until the peak load was attained. For each increment of load the DM gauge data were recorded and the crack pattern was traced and marked.

2.4. MECHANICAL PROPERTIES

The results of the material control tests are summarised in Table 3 and full details of the strength tests can be obtained from Voo et al. [6] and Voo [7]. The mean compressive strength ( $f_{cm}$ ) was determined from six 200 mm high by 100 mm diameter cylinders stressed under load control at a rate of 20 MPa/min according to AS1012.9 [8]. The ends of the cylinders were ground flat. The cube compressive strength ( $f_{cu}$ ) was determined from 70 mm cubes stressed under load control at a rate of 20 MPa/min.

The modulus of elasticity ( $E_c$ ) and the Poisson's ratio ( $\nu$ ) were obtained from stress-strain tests on 200 mm high by 100 mm diameter cylinders tested under circumferential displacement control at a rate of between 25  $\mu\epsilon$ /min and 150  $\mu\epsilon$ /min over a period of approximately two hours.

The split cylinder tensile strength ( $f_{sp}$ ) was obtained from tests on six 200 mm high by 100 mm diameter cylinders loaded at 1.0 MPa/min via a 10 mm wide loading strip. The notched three point flexural tension strength ( $f_{fp}$ ) was obtained from 100 mm square prisms spanning 400 mm with a notch depth of 25 mm. The specimens were counter balanced to eliminate the effect of the self-weight on the fracture measurement and the specimens were controlled under crack mouth opening displacement (CMOD) at a rate of 500  $\mu\epsilon$ /min. The fracture energy ( $G_f$ ) was obtained from notched three point bending tests with either the total area under the load versus displacement or the load versus CMOD curves divided by the net cross-sectional area of the specimens.

Table 3: Mechanical properties

Specimen	SB1	SB2	SB3	SB4	SB5	SB6	SB7
$E_c$ (GPa)	44	45	43	43	49	40	46
$\nu$	0.15	0.15	0.14	0.14	0.14	0.13	0.13
$f_{cm}$ (MPa)	161	160	149	164	171	157	169
$f_{cu}$ (MPa)	176	178	166	180	187	168	185
$f_{sp}$ (MPa)	19.2	20.9	21.9	18.0	22.4	18.3	23.5
$f_{fp}$ (MPa)	11.9	11.2	10.6	10.3	13.6	10.2	11.1
$f_{cf}$ (MPa)	29.8	26.4	23.2	14.8	26.3	25.2	23.8
$G_f$ (N/mm)	27.7	24.7	21.0	14.3	15.5	12.4	18.6
Flow (mm)	170	180	210	170	150	210	180



Figure 4: Specimen SB3 in testing frame (heavy structural laboratory of School of Civil and Environmental Engineering - University of New South Wales, Sydney, Australia)

Double punch tensile strength ( $f_{dp}$ ) tests were undertaken on 200 mm high by 100 mm diameter cylinders using a pair of 25 mm high by 25 mm diameter rigid steel circular punches on the top and bottom surface of the specimens and were loaded at 1 MPa/min. Equation as proposed by Chen and Yuan [9] is used to evaluate the double punch tensile strength.

### 3 TEST RESULTS AND OBSERVATIONS

The experimental results of the shear tests are summarised in Table 4, where  $P_{cr}$  is the first shear cracking load determined by visual observation of cracks on the specimens and  $P_u$  is the maximum or peak load recorded during the experiments. Specimen SB3 is the control specimen and it is used to compare the ultimate shear strength of the other six specimens.

Comparing the mean cylinder compression strengths with the double punch tensile strength (refer Table 3) for specimens SB1, SB2 and SB3 (the specimens with 2.5% of 13 mm straight fibre), the ratios of tensile strength is similar to that of the compressive strengths. A similar variation is also seen in the flexural tension strengths and fracture energies but, curiously, not in the split cylinder tension results. In Table 4 the experimental results are compared to that for specimens SB3 corrected for the variation in compressive strength.

In terms of the prestressing levels, the comparison presented in Table 4 indicates a 15% variation in strength due to the effect of prestressing. In terms of the quantity of the same type of fiber, Table 4 shows the comparative strength of specimen SB4 (with 1.25% fibres) was 30% lower than specimen SB3 (with 2.5% fibres).

For the test using different fibre types, Table 4 shows that the failure loads were lower with increasing quantities of the 30 mm end hooked fibres and reducing quantities of 13 mm straight fibres. This indicates that fibre fracture may have had a significantly greater influence for the longer end hooked fibres than for the short straight fibre.

Table 4: Experimental results

Beams No.	$P_{cr}$ (kN)	$P_u$ (kN)	$\frac{P_u}{P_{cr}}$	$\frac{P_u}{P_{u,SB3}} \cdot \frac{f_{cm,SB3}}{f_{cm}}$
SB1	300	860	2.9	0.93
SB2	400	994	2.5	1.08
SB3*	300	856	2.9	1.00
SB4	300	673	2.2	0.71
SB5	400	880	2.2	0.90
SB6	250	660	2.6	0.73
SB7	350	800	2.3	0.82

This is further evidenced by the lower fracture energies measured in the control specimens for increasing end hooked fibre to straight fibre ratios (refer Table 3).

A comparison of the crack patterns (Figure 5) show all the girders behaved in a similar manner with the diagonal shear cracking initiated in the web regions of each of the shear spans. The diagonal cracks then multiplied and propagated toward the top flange and smeared across the spans with increasing load. Finally, failure resulted from tensile fracture across a single, dominant, crack or from a coalescence of cracks leading to the formation of a dominant crack.

The raw data for the Demec strain readings for the seven shear beams are given in Voo et al. [6] and Voo [7]. The load-deflection curves of specimens SB1 to SB7 are given in Figure 6. In this

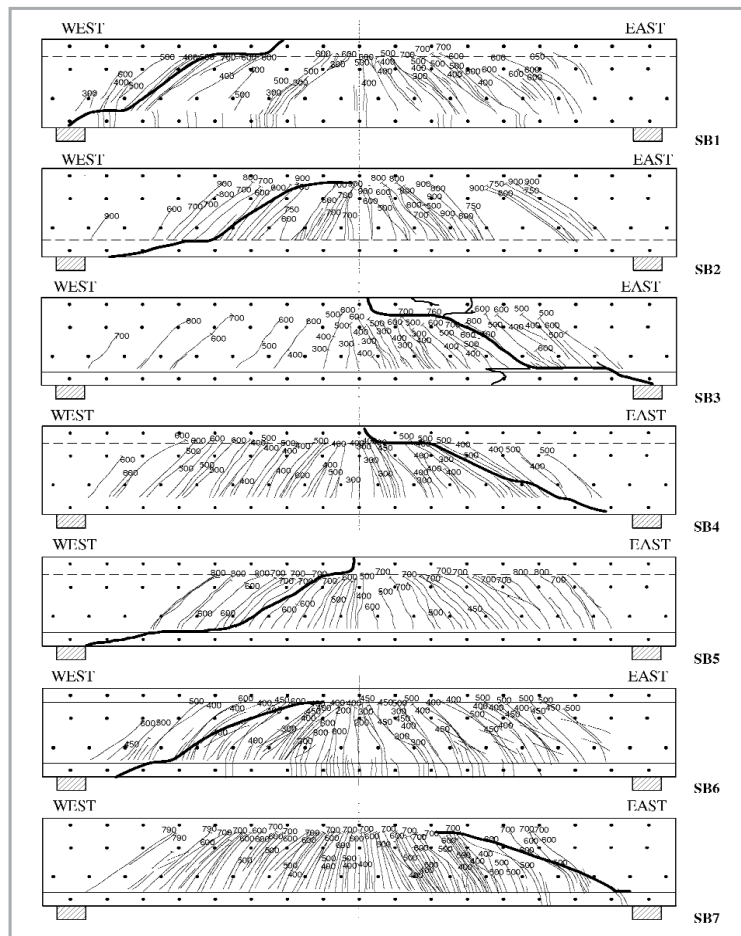


Figure 5: Crack patterns for specimens SB1 to SB7

## SHEAR STRENGTH OF 160 MPa STEEL FIBRE REINFORCED REACTIVE POWDER CONCRETE BRIDGE GIRDERS WITHOUT STIRRUPS

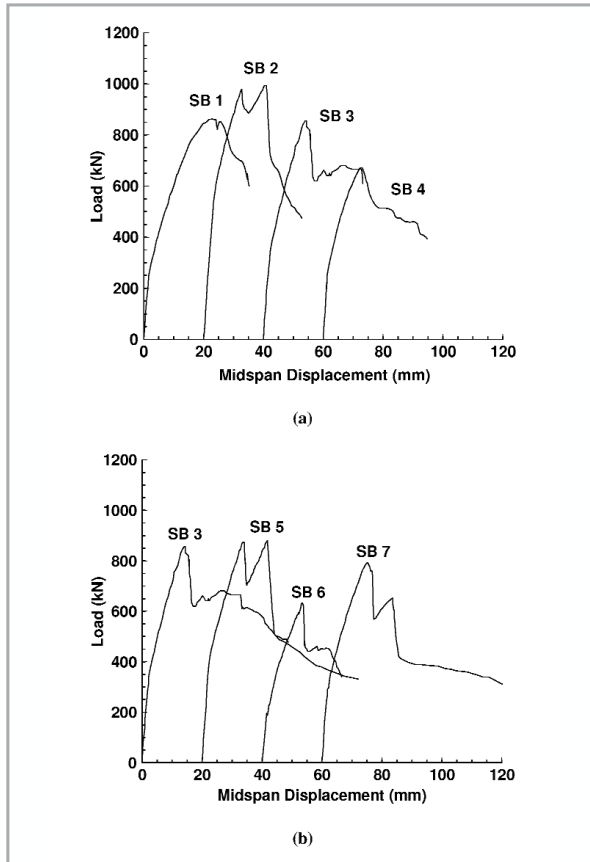


Figure 6: Load vs midspan deflection of SB1 to SB4 and SB3, and SB5 to SB7

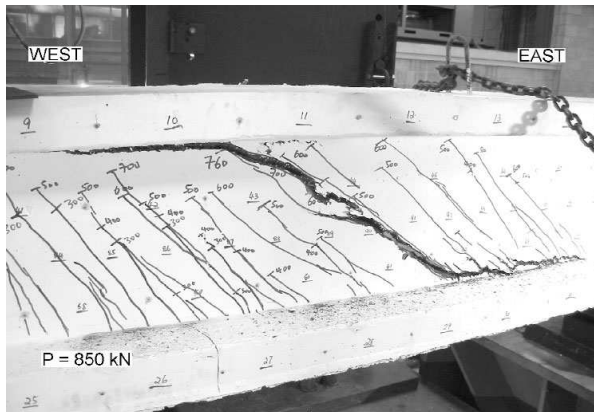


Figure 7: SB3: major diagonal shear crack at  $P = 850$  kN

paper, experimental observations for selected specimen, SB3 is reported. The first diagonal shear cracking was observed at a load of 300 kN. Figure 7 shows as the loading was increased a number of diagonal shear cracks formed and the cracks were smeared across the span. At 850 kN a major diagonal crack formed in the east span. The peak load was 856 kN. After the peak load, the diagonal crack opened considerably and the load reduced.

Figure 8 was taken at a post peak load of 700 kN with all fibres being pulled out along the crack plane. Figure 9 shows that at the post peak load of 600 kN, the top flange of the girder is rotated at two distinct locations with the crack width of the major

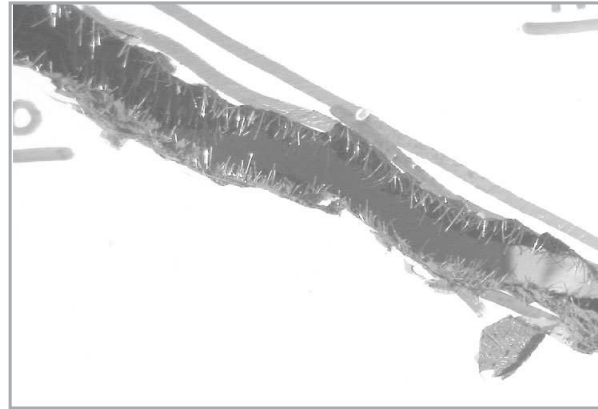


Figure 8: SB3: fiber pullout at the critical diagonal crack at post peak load of 700 kN

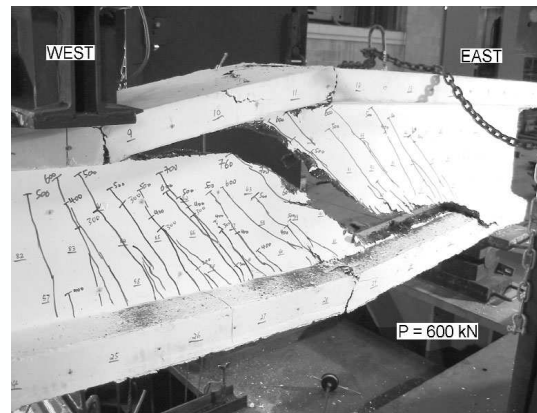


Figure 9: SB3: flange rotation at post peak  $P = 600$  kN

diagonal crack being over 100 mm. Testing of specimen SB3 was concluded when the post peak load had reduced to 320 kN.

#### 4 ANALYSIS OF RESULTS

Comparison of the crack patterns in the shear beams show that the quantity of fibres, type of fibre and prestressing level only marginally affected the shear cracking load ( $P_{cr}$ ) but did have a significant influence on the rate of crack growth. After the initial cracking of the specimens, the cracks propagated at a faster rate in specimen SB4, the specimens with the lowest quantity of steel fibres.

Figure 6a compares the load versus mid-span deflection of specimens SB1, SB2, SB3 and SB4. The figure shows that at different levels of prestressing, not only did the ultimate shear strength of the specimens increase with increasing prestress but the prestress also influenced the stiffness of the girders. Comparison of specimen SB1 (i.e. with no prestressing) and SB2 (i.e. with average 14.2 MPa prestress in the web) shows the ultimate shear strength increased by approximately 16%.

In terms of varying the ratio of fiber quantities in the cocktail mixes, Figure 6b compares the load versus mid-span displacement of specimens SB3, SB5, SB6 and SB7. The ultimate shear strength and the stiffness of the specimens decreased as the quantity of the straight steel fibres was reduced.

The horizontal strains measured at the top and bottom flanges of selected specimen (i.e. SB3) presented in Figure 10. Full experimental data of the DM gauge readings can be

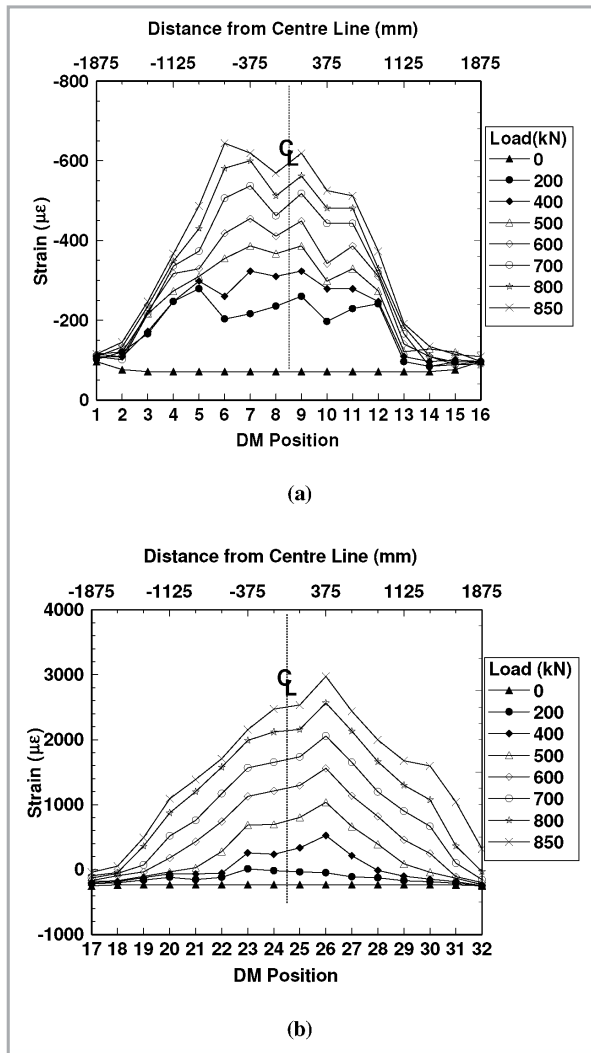


Figure 10 - SB3: (a) strains in top flange (DMs 1 to 16) and strain in bottom flange (DMs 17 to 32), includes prestrain.

obtained from Voo et al. [6] and Voo [7]. The measured compressive strains were of the order of  $600 \mu\epsilon$  to  $800 \mu\epsilon$ , which are equivalent to compressive stresses of 27 MPa to 36 MPa. This indicates that crushing of the top flanges was not an issue. The maximum tension strains at the bottom flange were  $2500 \mu\epsilon$  to  $4500 \mu\epsilon$ . This indicates that the strands remained in the elastic range and yielding of the tension reinforcement was also not an issue (strand yield strain,  $\epsilon_{py} = 8970 \mu\epsilon$ ).

## 5 CONCLUSIONS

Seven reactive powder concrete prestressed girders without stirrups were tested to study the capacity of steel fibre reinforced RPC beams in shear. The test variables were the quantity and type of fibres and the prestress. The steel fibers used in the tests consisted of either 13 mm straight fibres and/or 30 mm end-hooked fibres. All the tested specimens had the same cross-section and were subjected to mid-point loading over a shear span of 2 meter. The shear span to effective depth ratio for the beams was 3.33.

From the experimental study the following conclusions are drawn:

I. The quantity of fibres and type of fibres used in the concrete mix does not significantly affect the cracking

load but has a significant influence on the rate of crack propagation and on the failure loads.

II. At the peak load, many fine cracks had formed in the web, with the cracks well distributed through the shears spans. The failure loads were more than twice the cracking loads. ■

## REFERENCES

- [1] Richard, P., and Cheyrezy, M.H., "Reactive Powder Concretes with High Ductility and 200-800 MPa Compressive Strength", *ACI*, SP-144(24), San Francisco, CA, pp: 507-518, 1994.
- [2] Richard, P., and Cheyrezy, M., "Composition of Reactive Powder Concretes", *Cement and Concrete Research*, Vol. 25, No. 7, pp: 1501-1511, 1995.
- [3] AS1311, "Steel Tendons for Prestressed Concrete - 7-Wire Stress-Relieved Steel Strand for Tendons in Prestressed Concrete", *Standards Australia*, 1987.
- [4] AS3972, "Portland and Blended Cements", *Standards Australia*, 1997.
- [5] ASTM C-230, "Standard Specification for Flow Table for Use in Tests of Hydraulic Cement", *ASTM International*, 2003.
- [6] Voo, J.Y.L, Foster, S.J. and Gilbert, R.L., "Shear Strength of Fibre Reinforced Reactive Powder Concrete Girders without Stirrups", UNICIV Report R-421, The University of New South Wales, School of Civil and Environmental Engineering, Kensington, Sydney, Australia, November, ISBN: 85841 388 4, 131 pp., 2003.
- [7] Voo, Y. L., "An Investigation into the Behaviour of Prestressed Reactive Powder Concrete Girders Subject to Non-Flexural Actions", *PhD. Thesis*, School of Civil and Environmental Engineering, The University of New South Wales, Sydney, Australia, May, 313 pp., 2004.
- [8] AS1012.9, "Determination of the Compressive Strength of Concrete Specimens", *Standards Australia*, 1986.
- [9] Chen, W.F., and Yuan, R.L., "Tensile Strength of Concrete: Double-Punch Test", *Journal of the Structural Division*, ASCE 106, pp: 1673-1693, 1980.

## NOMENCLATURE

$E_c$	composite modulus of elasticity
$f_{cf}$	composite flexural tensile strength
$f_{cm}$	mean composite cylinder compressive strength
$f_{cu}$	composite cube compressive strength
$f_{dp}$	composite double punch tensile strength
$f_{sp}$	composite split-cylinder tensile strength
$G_f$	fracture energy determined from three point flexural tensile test
$G_F$	fracture energy determined from uniaxial tension tests
$P_{cr}$	shear cracking load
$P_u$	maximum load
$\nu$	composite Poisson's ratio
$\sigma_{av}$	average axial stress at fracture
$\sigma_{bot}$	extreme fibre stress at bottom of beam at transfer of prestress
$\sigma_{top}$	extreme fibre stress at top of beam at transfer of prestress